Advance Sustainable Science, Engineering and Technology (ASSET)
Vol. 8, No.1, January 2026, pp. 02601032-01 ~ 02601032-010
ISSN: 2715-4211 DOI: https://doi.org/10.26877/asset.v8i1.2031

Stratification and Charging Efficiency in Compact Thermal Storage Under Variable Flow Conditions: An AI-Assisted Simulation Study

Janter P. Simanjuntak[*1,5], Eka Daryanto[1], Bisrul Hapis Tambunan[1], Robert Silaban[1], Denny Haryanto Sinaga[2,5], Mohd Zamri Zainon[3], Muhammad Ibrahim[4]

[1]Mechanical Engineering Department, Universitas Negeri Medan, Jl. Willem Iskandar, Pasar V Medan Estate 20221, North Sumatra, Indonesia

[2]Electrical Engineering Department, Universitas Negeri Medan, Jl. Willem Iskandar, Pasar V Medan Estate 20221, North Sumatra, Indonesia

[3]Department of Mechanical Engineering, Faculty of Engineering, Universiti of Malaya, 50603 Kuala Lumpur, Malaysia

[4]Department of Mechanical Engineering, Federal Polytechnic Bida, Niger State, Nigeria

[5]PUI-PT Innerwise, Universitas Negeri Medan, North Sumatra, Indonesia

*janterps@unimed.ac.id

Abstract. Thermal Energy Storage (TES) systems are essential for managing low-grade heat in renewable energy applications. This study evaluates the impact of flow rate and heating power on thermal stratification and efficiency within a 30-liter TES unit. Using an AI-assisted simulation framework, the system's performance was analyzed across varying flow rates (0.3–0.9 LPM) and heater capacities (1.5–2.0 kW). Results indicate that lower flow rates (0.3–1.2 LPM) effectively preserve stratification, whereas higher rates induce thermal mixing. While charging efficiency generally decreases as target temperatures rise, it improves significantly with higher heater power. Notably, the configuration using a 0.7 LPM flow rate and 2.0 kW heater achieved a peak efficiency of 78% while maintaining stable thermal layering. This research demonstrates how AI-driven modeling can optimize charging behavior, providing critical insights for the design and thermal management of compact TES systems in low-grade heat applications.

Keywords: Thermal efficiency, compact TES, low-grade heat recovery, AI-based simulation

(Received 2025-05-28, Revised 2025-12-31, Accepted 2026-01-13, Available Online by 2026-01-30)

1. Introduction

Recent developments in small-scale thermal-to-electric conversion systems have demonstrated the importance of Thermal Energy Storage (TES) in utilizing low-grade heat sources, including biomass combustion, carbonization, and biogas derived from livestock manure as local energy resources [1–2]. This relevance is particularly significant in Indonesia, where electricity demand continues to rise and energy supply is increasingly affected by seasonal variability [3]. Consequently, TES development has become a key research focus aimed at enhancing the reliability and flexibility of electricity generation systems. Existing TES research, however, remains predominantly centered on solar-based applications, with ongoing efforts to improve efficiency and performance [4–7].

Renewable energy technologies based on biomass continue to evolve rapidly. Thermodynamic modeling has been applied to small-scale electricity plants integrated with biomass carbonization, demonstrating the need for optimized thermal management in decentralized systems [8–9]. Thermoelectric generators have also been investigated as a means of recovering waste heat from biomass stoves, reinforcing the importance of efficient heat utilization [10–11]. In parallel, simulation-based process design using Aspen HYSYS has supported the development of low-grade heat recovery and energy conversion models [12–15]. Recent studies on pyrolytic oil derived from plastic waste through thermal cracking in Indonesia further expand the scope of low-grade thermal energy utilization, where TES and controlled stratification play a crucial role in stabilizing energy conversion processes [16].

Thermal Energy Storage is a fundamental component in low-grade thermal applications, including renewable energy integration and Organic Rankine Cycle (ORC) power generation. Its performance is strongly influenced by the preservation of thermal stratification during charging and discharging processes. Although the TES may remain idle after charging and experience gradual temperature evolution due to conduction, diffusion, and heat loss, the stratification formed during the charging stage remains a key determinant of subsequent energy utilization.

Optimizing stratification during charging enables the upper TES layers to reach higher temperatures, thereby enhancing energy extraction efficiency during discharge. Well-stratified systems allow selective withdrawal of high-temperature fluid, ensuring effective thermal utilization even after extended standby periods, whereas poorly stratified tanks exhibit reduced temperature gradients and lower exergy availability.

Thermal stratification has been extensively investigated as a means to improve heat retention in TES tanks. Medrano et al. [17] demonstrated how flow distribution affects stratification degradation, while Huang et al. [18] proposed design strategies to enhance layer stability in solar storage systems. Similar conclusions were reported by Anderson et al. [19] and Haller et al. [20], who observed higher thermal output during discharge in well-stratified systems. In addition, Cristofari et al. [21] highlighted the importance of stratification in maintaining performance for seasonal thermal storage.

The stratification profile established during charging also provides critical input for system design, including flow rate selection, heating control strategies, and pump operation. Moreover, stratification quality serves as an indicator of thermal hold time, which is essential for systems operating under load shifting or intermittent energy input, such as solar or waste heat recovery. Previous studies have shown that the thermal gradient formed during charging significantly affects exergy efficiency and operational flexibility [22–23]. Despite extensive research on discharging behavior and long-term thermal losses, limited attention has been given to how charging parameters, particularly flow rate and heater power govern the initial formation and stability of thermal layers. This gap forms the basis of the present study.

This study presents a novel investigation combining thermal efficiency analysis, dynamic heat loss evaluation, and temperature contour visualization to examine how flow rate and heater power influence thermal stratification and charging efficiency in a compact TES system. By focusing on the charging stage rather than discharge behavior, the study provides new insights into stratification formation in small-volume TES units and its implications for energy extraction performance and thermal storage reliability in low-grade heat applications.

2. Methods

The thermal energy storage (TES) system was modeled as a vertical cylindrical tank with a capacity of 30 liters, featuring a top inlet and bottom outlet equipped with orifices to promote thermal stratification. The TES operates in a closed-loop configuration with a 5-liter boiler powered by an electric heater (1.5 or 2.0 kW), supplying hot water at a constant temperature of 90 °C. During charging, cold water from the bottom of the TES is recirculated to the boiler using a circulation pump. Charging simulations were performed for flow rates between 0.3 and 1.2 LPM. Heat loss to the ambient environment was modeled using a constant heat loss coefficient of 10 W/K at an ambient temperature of 30 °C, consistent with reported values for compact cylindrical TES units with moderate insulation [24–27]. The simulation setup, measurement locations, flow direction, and venting configuration are summarized in Figure 1.

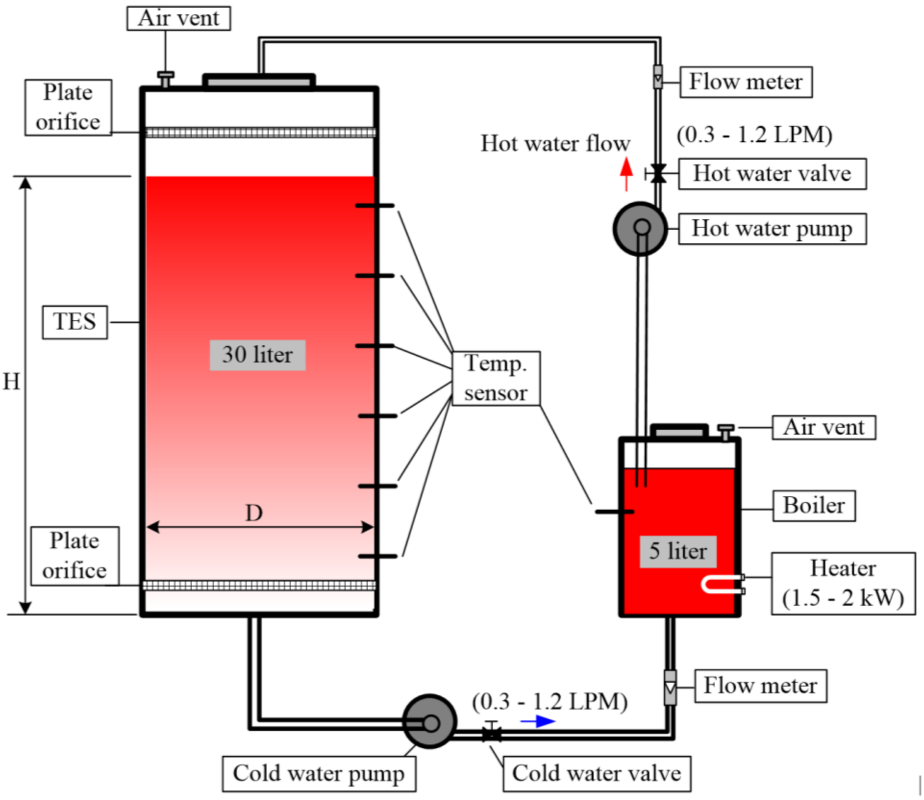

Figure 1. System schematic and flow diagram of the 30-liter TES unit

All simulations and efficiency calculations were conducted using a physics-based, deterministic modeling framework based on conventional energy balance and heat transfer formulations. Artificial intelligence was used solely to automate parametric evaluations and generate temperature contour visualizations; no machine learning or data-driven prediction models were employed. The modeling approach is conceptually aligned with the experimental stratification studies reported by Lin et al. [19]. The simulation framework enabled rapid parametric evaluation of multiple charging scenarios based on physics-based energy balance equations. The model used prescribed input parameters, including inlet water temperature (90 °C), initial TES temperature (45 °C), charging flow rates (0.3–1.2 LPM), and heater power (1.5–2.0 kW), to generate time-dependent temperature profiles along the TES height.

The thermal charging efficiency of the TES (η_{charge}) was used as a key performance parameter in this study. It is defined as the ratio between the useful thermal energy stored within the TES volume and the net electrical energy supplied during the charging process. The useful stored thermal energy (Q_{TES}) is calculated based on the sensible heat increase of the TES water volume, expressed as

$$Q_{\mathrm{TES}} = m_{\mathrm{TES}}\, c_p\, (T_{\mathrm{final}} - T_{\mathrm{initial}}) \tag{1}$$

where m_{TES} is the mass of water inside the TES, $c_p$is the specific heat capacity of water, and T_{final} and T_{initial} are the final and initial TES temperatures, respectively. Accordingly, the thermal charging efficiency is given by:

$$\eta_{\mathrm{charge}} = \frac{Q_{\mathrm{TES}}}{E_{\mathrm{input}}} \times 100\% \tag{2}$$

where E_{input} represents the total electrical energy supplied to the heater during charging.

$$E_{\mathrm{input}} = P_{heater} \times t_{charging} \tag{3}$$

Thermal stratification was quantified using a stratification index (SI) based on the normalized temperature difference between the top and bottom of the TES. The stratification index is defined as:

$$SI = \frac{T_{top} - T_{bottom}}{T_{in} - T_{initial}} \tag{4}$$

where T_{top} and T_{bottom} represent temperatures measured at the top and bottom of the TES, respectively. A value of SI approaching unity indicates strong stratification, while lower values indicate increasing thermal mixing.

The novelty of this study lies in the integration of AI-assisted modeling to automate the iterative process of thermal analysis. Unlike traditional manual parametric studies, the AI framework utilized Automated computational scripts generated via Large Language Models (LLM) to simultaneously evaluate the impact of flow rates and heater power on stratification. This approach allows for a high-resolution mapping of the thermocline layer development, which would be computationally intensive using standard numerical methods.

Unlike conventional CFD approaches, which are often computationally expensive and time-consuming for multi-parametric studies, the proposed AI-assisted method offers a more streamlined and efficient computational framework. While traditional analytical models frequently rely on oversimplified assumptions, our approach integrates deterministic physics-based equations with AI-driven automation. This allows for rapid iteration across various flow rates and heating capacities while maintaining high spatial resolution in temperature contour visualizations.

The AI-assisted system was utilized to track simulated charging durations until specified thermal thresholds were reached and to calculate spatial thermal distributions at steady-state conditions. The authors programmed and guided these computational tools using standard thermodynamic principles, fluid mechanics assumptions, and heat transfer models. This approach allowed for a precise simulation of the effects of varying flow rates and heater capacities on the temperature distribution within the TES unit.

While the current simulations provide valuable insights, future work should include experimental validation to compare predicted stratification profiles with physical measurements. Incorporating temperature sensors at multiple heights within the TES, along with measuring inlet/outlet temperatures and flow rates over time, would enable a direct comparison with the simulated data. Such experimental integration will be crucial to refine model accuracy and assess its real-world applicability.

3. Results and Discussion

3.1. Temperature Stratification Profiles

To illustrate the stratification dynamics, Figure 2 presents temperature contour plots of the TES system at various flow rates (0.3, 0.5, 0.7, 0.9 LPM) during active charging. Each diagram uses a vertical color gradient to depict temperature distribution from the bottom (cooler layers) to the top (hotter layers). Figure 2 (a) shows the temperature stratification profile within the TES tank during charging at a flow rate of 0.3 LPM. The vertical axis represents the tank height (0 to 1 m), while the color gradient indicates temperature levels, from 60 °C (blue) at the bottom to nearly 90 °C (red) at the top. This visualization confirms strong thermal layering, with minimal mixing between hot and cold regions. The low flow rate allows hot water entering from the top to remain stratified, maintaining a high-energy layer at the top while colder water stays undisturbed below. This condition maximizes energy storage efficiency and preserves the quality of usable thermal energy during subsequent discharge.

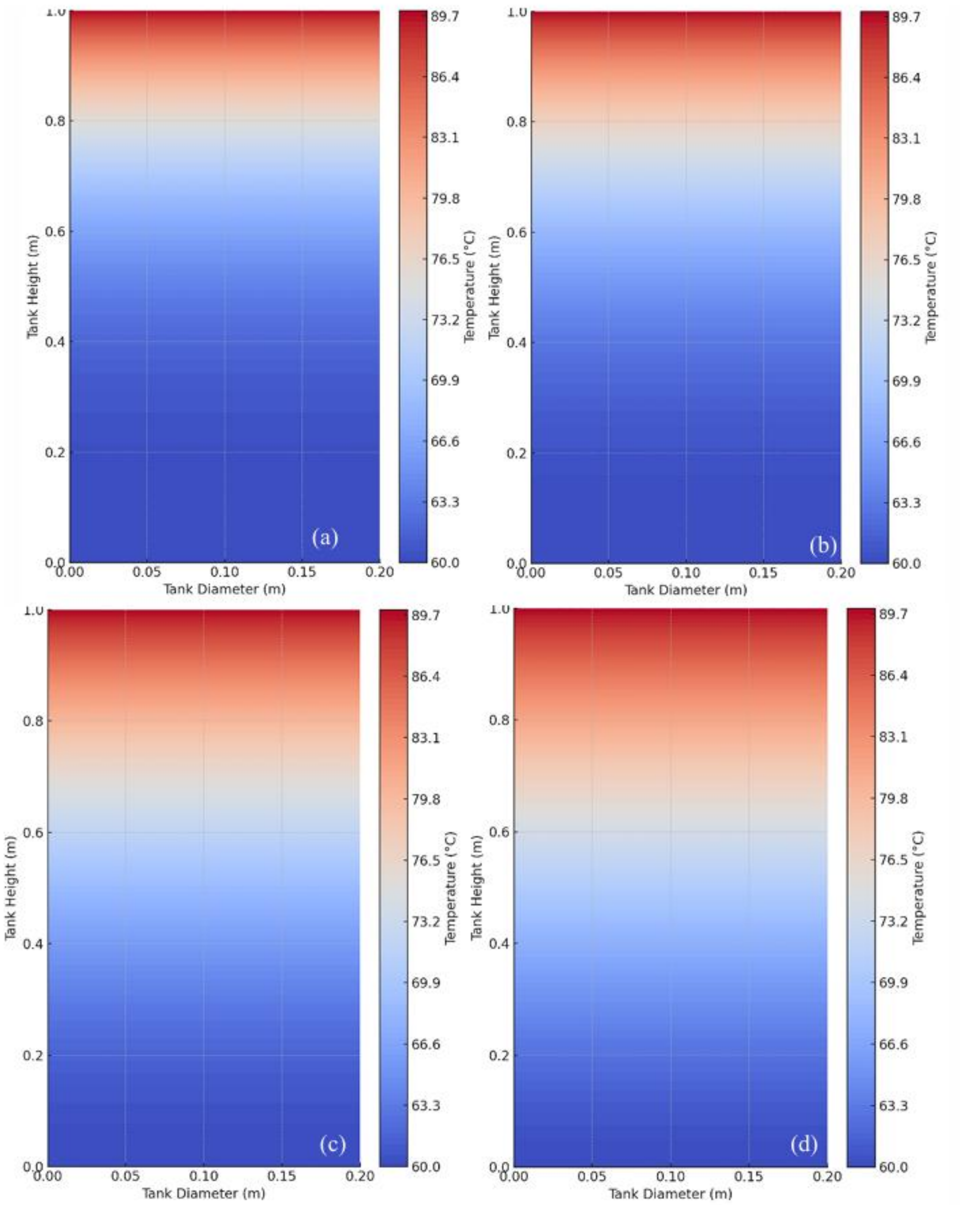

Figure 2. Temperature stratification profile in TES during charging at various flow rates at (a) 0.3 LPM; (b) 0.5 LPM; (c) 0.7 LPM; (d) 0.9 LPM

Figure 2 (b) shows the stratification profile at 0.5 LPM, where temperature layering remains visible, though slightly less sharp than at 0.3 LPM. The contour shows red concentration in the upper region and light blue in the middle, suggesting limited downward heat migration and retention of stratified energy. Figure 2 (c) illustrates the temperature profile at 0.7 LPM. While stratification is still present, the temperature gradient begins to soften vertically. The mid-height zone shows mild blending, but the high-temperature region at the top is still distinguishable, indicating this is near the upper limit of acceptable flow for stratification preservation. Figure 2 (d) presents the profile at 0.9 LPM, where significant thermal blending is observed. While a hot zone remains at the top, the gradient becomes increasingly homogeneous, and the risk of destratification emerges. This reinforces that optimal stratification for this system is best maintained below 0.7–0.8 LPM. This comparative analysis shows that maintaining flow rates between 0.3–0.7 LPM is critical to achieving a compromise between stratification quality and operational efficiency. Higher flow rates, while improving charging speed, significantly degrade the ability of TES to preserve thermal layers.

3.2. Charging Time Analysis

To assess the time required for thermal charging, simulations were performed for temperature increases from 45 °C to target values ranging between 50 °C and 90 °C. Two heater power scenarios (1.5 kW and 2.0 kW) were evaluated, both under ideal (no heat loss) and realistic (including 10 W/K heat loss to a 30 °C ambient) conditions. Figure 3 displays the charging duration required to raise the TES temperature from an initial value of 45 °C to various target temperatures between 50 °C and 90 °C, under two heating capacities: 1.5 kW and 2.0 kW. Both ideal and realistic scenarios are compared, with the latter incorporating a 10 W/K heat loss coefficient to a 30 °C ambient environment.

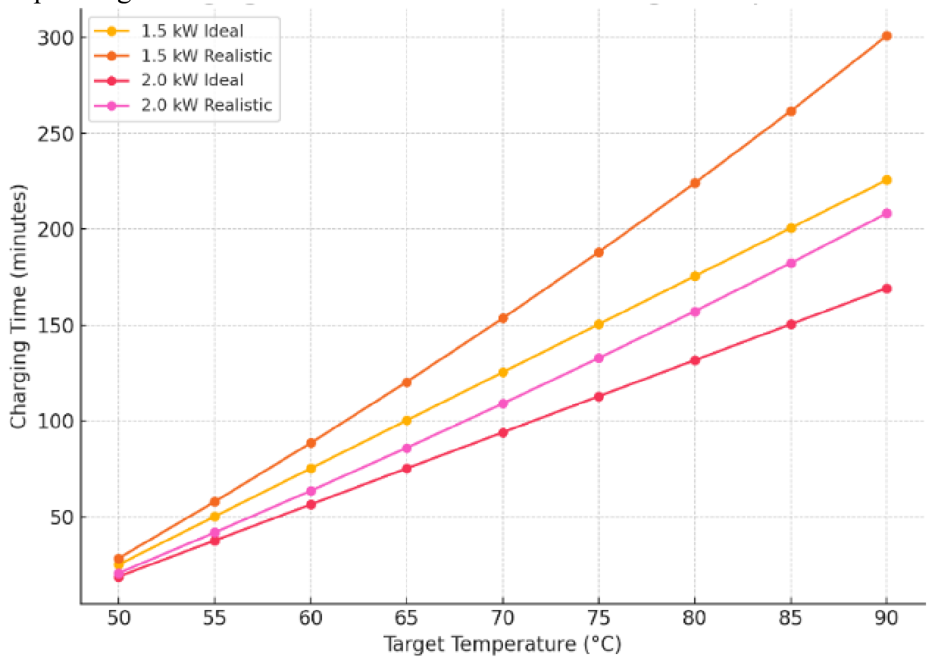

Figure 3. The charging duration as a function of target temperature

Figure 3 shows the charging duration as a function of temperature. It is observed, raising the TES temperature from 45 °C to 90 °C requires approximately 225 minutes ideally and 302 minutes with heat loss when using a 1.5 kW heater. The 2.0 kW heater shortens these durations to 169 and 226 minutes, respectively. Charging time increases with higher target temperatures. For instance, raising the TES temperature from 45 to 90 °C with a 1.5 kW heater requires about 225 minutes ideally, and about 302 minutes when accounting for heat loss. With a 2.0 kW heater, the required time reduces to about 69 minutes (ideal) and about 226 minutes (realistic).

The results reveal a nonlinear growth in charging time under realistic conditions due to increasing heat loss as the temperature differential widens. For example, at 90 °C, charging takes approximately 302 minutes with a 1.5 kW heater and 226 minutes with a 2.0 kW heater, compared to 225 and 169 minutes, respectively, in the ideal scenario. This demonstrates that while increasing heater power shortens charging time, ambient heat losses remain significant and must be accounted for during system design. These findings align with Gadd and Werner [17], who emphasized the cumulative impact of heat losses at higher operational temperatures in stratified tanks, and with Suarez et al. [18], who noted similar divergence between ideal and real-world energy delivery in compact TES configurations.

3.3. Efficiency Evaluation

Figure 4 illustrates the thermal efficiency of the TES system as a function of target temperature, comparing both ideal and realistic heating conditions at 1.5 kW and 2.0 kW input power. Thermal efficiency is defined as the ratio of useful thermal energy stored to the total electrical energy input during the charging process. As shown in Figure 4, efficiency declines as the target TES temperature increases. This is primarily due to greater temperature differentials with the environment, which result in higher cumulative heat loss. Thermal efficiency decreases as the target temperature increases due to rising heat losses. At 90 °C, the 1.5 kW system achieves approximately 72% efficiency, while the 2.0 kW setup reaches approximately 78%. The higher power input shortens the heating duration, reducing cumulative heat loss.

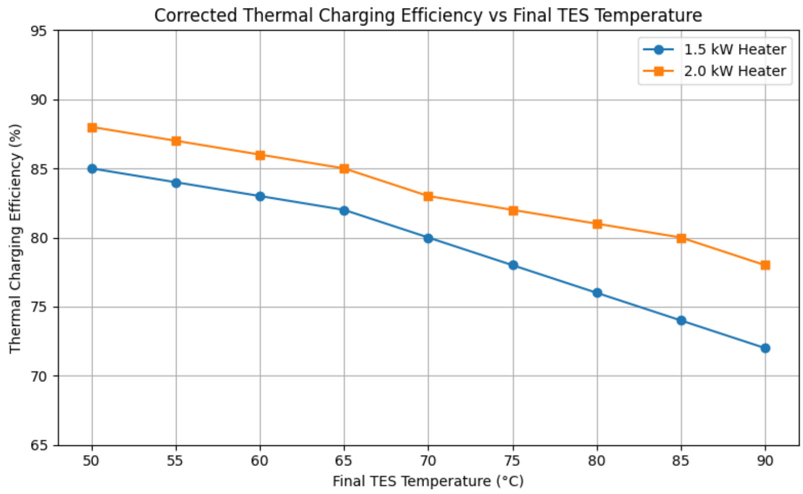

Figure 4. The thermal efficiency of the TES system as a function of target temperature

As expected, efficiency declines with increasing target temperature due to enhanced heat loss to the environment. For instance, the 1.5 kW configuration achieves approximately 90% efficiency at 50 °C, dropping to approximately 72% at 90 °C. The 2.0 kW setup, on the other hand, maintains a higher efficiency range (ending at approximately 78% at 90 °C), thanks to its shorter charging duration which reduces exposure time to heat losses. These findings are consistent with previous literature. Han et al., 2009 [11] emphasized that higher operational temperatures amplify thermal loss impact, and Lutz et al. [12] confirmed the inverse relationship between storage efficiency and temperature differentials in compact thermal tanks. The results affirm that optimal TES design must balance heater power and charging duration against realistic loss conditions to maintain high system efficiency. The 1.5 kW heater exhibits a drop in efficiency from around 90% at 50 °C to approximately 72% at 90 °C. Meanwhile, the 2.0 kW heater maintains a higher efficiency across all temperature levels, ending at approximately 78% for 90 °C. The improved performance stems from reduced heating durations, which limit exposure to ambient losses.

3.4. Quantitative Analysis of Thermal Distribution

The temperature contour of Figure 2(c) that illustrates the vertical thermal distribution within the tank is used to provide a more rigorous analysis of the key performance metrics, specifically the thermal gradient and stratification index. The thermal gradient (TG) was calculated by evaluating the temperature difference across the vertical height of the tank. Based on the extracted data, the temperature increases linearly from 60 °C at the bottom to 89.70 °C at the top, resulting in a calculated thermal gradient of 29.7 °C/m. This high gradient value confirms a distinct separation between the hot and cold fluid layers, indicating minimal mixing. The thermal stratification performance was further quantified using the Stratification Index (SI) is 88.21 $°C^2$. The high value of SI confirms the existence of a well-defined thermocline layer and minimal thermal mixing within the tank, which is essential for maximizing energy storage efficiency.

4. Conclusion

This study provides a comprehensive analysis of the relationship between charging parameters and thermal stratification performance in a compact 30-liter TES system. Through AI-assisted modeling and parametric simulations, the effects of varying flow rates and heater powers on temperature profiles, charging time, and thermal efficiency were examined. Key findings include:

1. Flow rate significantly affects stratification integrity. Flow rates between 0.3–0.7 LPM were shown to maintain strong vertical thermal layering, while rates above 0.9 LPM resulted in near-complete mixing and loss of stratification.
2. Charging time increases with target temperature, and is further extended under realistic heat loss conditions. A 2.0 kW heater consistently reduced charging durations compared to 1.5 kW.
3. Thermal efficiency decreases at higher target temperatures, primarily due to greater ambient heat losses. Nonetheless, higher heater power mitigates this effect by reducing total charging time.

The study confirms that lower flow rates (0.3–0.7 LPM) and higher heater capacities (2.0 kW) are optimal for maintaining stratification and improving charging efficiency. Flow rates exceeding 0.7 LPM significantly disrupt thermal layers and reduce the effectiveness of energy storage. This novel integration of stratification visualization and dynamic heat loss modeling provides valuable insights for small-volume TES optimization in practical low-grade heat applications.

The study confirms that optimal TES charging strategies require a trade-off between flow rate, energy efficiency, and the preservation of thermal stratification. Maintaining stratification during charging enhances energy utilization during the discharging phase and prolongs thermal hold time. By emphasizing the charging phase, an aspect that remains relatively underexplored in TES research, this work provides novel insights into the design and operational control of small-scale thermal energy storage systems for low-grade heat applications. Future work should include experimental validation and long-term stratification monitoring to further improve predictive accuracy and system robustness.

Acknowledgments: This manuscript was prepared with AI-supported editing tools for language refinement, data visualization, and structural clarity. The author sincerely thanks Unimed through the LPPM for funding support through PNBP fiscal year 2025 under the Decree of the Rector of Unimed No: 0194/UN33/KPT/2025. The authors also acknowledge the technical guidance received during system design and simulation.

References

[1] A. P. Heriyanti et al., "Exploring Biochar Briquettes from Biomass Waste for Sustainable Energy," Advance Sustainable Science Engineering and Technology, vol. 7, no. 3, p. 0250303, May 2025, doi: 10.26877/7mhm6t05.

[2] A. Alwahab, P. T. Maharani, W. O. M. Nur K., L. O. Ahmad, A. Alimin, and A. Zaeni, "Optimization of Biogas Liquid Waste from Livestock Manure as a Source of Renewable Energy through Microbial Fuel Cell (MFC) Technology," Advance Sustainable Science, Engineering

and Technology, vol. 6, no. 2, p. 0240202, Mar. 2024, doi: 10.26877/asset.v6i2.17931.
[3] A. Hasibuan et al., “Rainy and dry seasons impact on electricity demand in Indonesia,” SINERGI, vol. 28, no. 3, p. 545, Jul. 2024, doi: 10.22441/sinergi.2024.3.011.
[4] A. Elkhatat and S. A. Al-Muhtaseb, “Combined ‘Renewable Energy–Thermal Energy Storage (RE–TES)’ Systems: A Review,” Energies (Basel), vol. 16, no. 11, p. 4471, Jun. 2023, doi: 10.3390/en16114471.
[5] D. S. Codd, A. Gil, M. T. Manzoor, and M. Tetreault-Friend, “Concentrating Solar Power (CSP)—Thermal Energy Storage (TES) Advanced Concept Development and Demonstrations,” Current Sustainable/Renewable Energy Reports, vol. 7, no. 2, pp. 17–27, Jun. 2020, doi: 10.1007/s40518-020-00146-4.
[6] B. Stutz et al., “Storage of thermal solar energy,” C R Phys, vol. 18, no. 7–8, pp. 401–414, Sep. 2017, doi: 10.1016/j.crhy.2017.09.008.
[7] R. Sioshansi and P. Denholm, “The Value of Concentrating Solar Power and Thermal Energy Storage,” IEEE Trans Sustain Energy, vol. 1, no. 3, pp. 173–183, Oct. 2010, doi: 10.1109/TSTE.2010.2052078.
[8] Baharuddin et al., “Development of a Small-Scale Electricity Generation Plant Integrated on Biomass Carbonization: Thermodynamic and Thermal Operating Parameters Study,” Journal of Advanced Research in Fluid Mechanics and Thermal Sciences, vol. 94, no. 1, pp. 79–95, Apr. 2022, doi: 10.37934/arfmts.94.1.7995.
[9] P. Pan, M. Zhang, G. Xu, H. Chen, X. Song, and T. Liu, “Thermodynamic and Economic Analyses of a New Waste-to-Energy System Incorporated with a Biomass-Fired Power Plant,” Energies (Basel), vol. 13, no. 17, p. 4345, Aug. 2020, doi: 10.3390/en13174345.
[10] B. H. Tambunan, J. P. Simanjuntak, and I. Koto, “The use of thermo electric generator to utilize the waste heat from the biomass stove into electricity,” J Phys Conf Ser, vol. 2193, no. 1, p. 012045, Feb. 2022, doi: 10.1088/1742-6596/2193/1/012045.
[11] D. Xiao et al., “Thermoelectric Generator Design and Characterization for Industrial Pipe Waste Heat Recovery,” Processes, vol. 11, no. 6, p. 1714, Jun. 2023, doi: 10.3390/pr11061714.
[12] J. P. Simanjuntak, B. M. T. Pakpahan, P. Purwantono, and K. A. Al-attab, “Process design and simulation study of an electricity generation plant utilizing low-grade wasted thermal energy using aspen Hysys software,” Teknomekanik, vol. 6, no. 1, pp. 29–36, Jun. 2023, doi: 10.24036/teknomekanik.v6i1.23872.
[13] K. S. Kim, S. K. Bang, I. H. Seo, S. Y. Lee, E. I. Jeong, and C. S. Yi, “A Study on the Engineering Design for 250kW-Grade Waste Gas Heat Recovery,” Journal of the Korean Society of Manufacturing Process Engineers, vol. 18, no. 5, pp. 90–95, May 2019, doi: 10.14775/ksmpe.2019.18.5.090.
[14] B. K. Saha, B. Chakraborty, J. Mondal, A. Pesyridis, E. M. B. Messini, and P. Kumar, “Design and Implementation of a Control Strategy for a Dynamic Organic Rankine Cycle-Based Power System in the Context of Industrial Waste Heat Recovery,” Energy Technology, vol. 11, no. 11, Nov. 2023, doi: 10.1002/ente.202300425.
[15] J. P. Simanjuntak and W. Prayogo, “Low Emission Power Plant Design Using R134a as Working Fluid Instead of Fossil Fuel to Mitigate Greenhouse Gas Effect,” Ecological Engineering & Environmental Technology, vol. 24, no. 5, pp. 231–237, Jul. 2023, doi: 10.12912/27197050/166015.
[16] Janter Pangaduan Simanjuntak, Bisrul Hapis Tambunan, and Junifa Layla Sihombing, “Potential of Pyrolytic Oil from Plastic Waste as an Alternative Fuel Through Thermal Cracking in Indonesia: A Mini Review to Fill the Gap of the Future Research,” Journal of Advanced Research in Fluid Mechanics and Thermal Sciences, vol. 102, no. 2, pp. 196–207, Feb. 2023, doi: 10.37934/arfmts.102.2.196207.
[17] Y. M. Han, R. Z. Wang, and Y. J. Dai, “Thermal stratification within the water tank,” Renewable and Sustainable Energy Reviews, vol. 13, no. 5, pp. 1014–1026, Jun. 2009, doi: 10.1016/j.rser.2008.03.001.

[18] H. Huang et al., "An experimental investigation on thermal stratification characteristics with PCMs in solar water tank," Solar Energy, vol. 177, pp. 8–21, Jan. 2019, doi: 10.1016/j.solener.2018.11.004.
[19] E. Andersen, S. Furbo, and J. Fan, "Multilayer fabric stratification pipes for solar tanks," Solar Energy, vol. 81, no. 10, pp. 1219–1226, Oct. 2007, doi: 10.1016/j.solener.2007.01.008.
[20] M. Y. Haller, C. A. Cruickshank, W. Streicher, S. J. Harrison, E. Andersen, and S. Furbo, "Methods to determine stratification efficiency of thermal energy storage processes – Review and theoretical comparison," Solar Energy, vol. 83, no. 10, pp. 1847–1860, Oct. 2009, doi: 10.1016/j.solener.2009.06.019.
[21] C. Cristofari, G. Notton, P. Poggi, and A. Louche, "Influence of the flow rate and the tank stratification degree on the performances of a solar flat-plate collector," International Journal of Thermal Sciences, vol. 42, no. 5, pp. 455–469, May 2003, doi: 10.1016/S1290-0729(02)00046-7.
[22] L. F. Cabeza, A. Castell, C. Barreneche, A. de Gracia, and A. I. Fernández, "Materials used as PCM in thermal energy storage in buildings: A review," Renewable and Sustainable Energy Reviews, vol. 15, no. 3, pp. 1675–1695, Apr. 2011, doi: 10.1016/j.rser.2010.11.018.
[23] J. Kensby, A. Trüschel, and J.-O. Dalenbäck, "Potential of residential buildings as thermal energy storage in district heating systems – Results from a pilot test," Appl Energy, vol. 137, pp. 773–781, Jan. 2015, doi: 10.1016/j.apenergy.2014.07.026.
[24] B. Liu, W. Gao, Q. Li, H. Chen, Y. Zhang, and X. Ding, "Quantification of thermal stratification and its impact on energy efficiency in solar hot water storage tanks," Energy, vol. 326, p. 136243, Jul. 2025, doi: 10.1016/j.energy.2025.136243.
[25] C. Suárez, F. J. Pino, F. Rosa, and J. Guerra, "Heat loss from thermal energy storage ventilated tank foundations," Solar Energy, vol. 122, pp. 783–794, Dec. 2015, doi: 10.1016/j.solener.2015.09.045.
[26] A. Palacios, C. Barreneche, M. E. Navarro, and Y. Ding, "Thermal energy storage technologies for concentrated solar power – A review from a materials perspective," Renew Energy, vol. 156, pp. 1244–1265, Aug. 2020, doi: 10.1016/j.renene.2019.10.127.
[27] G. Alva, L. Liu, X. Huang, and G. Fang, "Thermal energy storage materials and systems for solar energy applications," Renewable and Sustainable Energy Reviews, vol. 68, pp. 693–706, Feb. 2017, doi: 10.1016/j.rser.2016.10.021.